Leadership in Sustainable Infrastructure
Leadership en Infrastructures Durables

Vancouver, Canada
May 31 – June 3, 2017/ *Mai 31 – Juin 3, 2017*

TOWARDS DEVELOPMENT LENGTH CRITERIA FOR PLAIN REINFORCING BARS IN TENSION

Poudyal, Umesh[1] and Feldman, Lisa R.[2,3]
[1] M.Sc. Student, Department of Civil, Geological, & Environmental Engineering, University of Saskatchewan, Canada
[2] Associate Professor, Department of Civil, Geological, & Environmental Engineering, University of Saskatchewan, Canada
[3] lisa.feldman@mail.usask.ca

Abstract: Thirty-five splice specimens reinforced with square or round plain bars cast in the bottom or top position were subjected to four-point loading to quantify the bond behaviour of plain reinforcing bars with concrete. Two of these splice specimens were intentionally cast with long lap splice lengths, such that a flexural failure was anticipated. All of the remaining specimens were designed to fail in bond. The failure of the two specimens that were designed to fail in flexure was of a ductile nature and included a long yield plateau. A moment curvature analysis was performed for all other specimens in which the compression zone was divided into 100 segments to calculate the tensile resistance of the reinforcement at the maximum load. This is the main basis for establishing provisions for lap splice and development length for bars in tension. The error in dividing the compression zone into 100 segments was negligible.

1 Introduction

Plain bars are no longer permitted to be used as reinforcement in Canada and the United States due to their limited bond strength capacity in comparison to modern deformed bars. As a result, there are no provisions for the bond evaluation of plain steel reinforcing bars in current editions of Canadian and American codes for reinforced concrete construction. In contrast, forensic engineers may be required to assess historical structures reinforced with plain bars and lack the necessary code provisions to confidently make such an assessment. ACI Committee 562 was organized in 2004 with the aim of developing a repair, evaluation, and rehabilitation code for existing structures. It is anticipated that bond provisions for plain bars will be included in a future edition of this code.

A review of the available literature revealed a limited number of works that can contribute to the development of code provisions for the bond and development of plain reinforcing bars in existing reinforced concrete structures. Hassan and Feldman (2010) conducted a limited study of 12 splice specimens to quantify the bond behaviour of plain steel bars. Based upon a comparison with data for specimens reinforced with modern deformed bars performed by Idun and Darwin (1995), they concluded that plain bars are 60% as effective in bond as modern deformed bars. Sekulovic MacLean and Feldman (2012) extended this investigation by casting an additional 15 specimens and studied the effect of casting position and bar shape (round versus square) on the bond of plain bars. They reported that square bars are less sensitive to casting position than round bars and reported that top cast factors of 0.3 and 0.6 for round bars and square bars, respectively, are appropriate. This finding was consistent with Chana's (1990) works in which it was reported that the bond of plain bars is more affected by casting position than that of deformed bars. These past works were not extended to determine the tensile resistance of reinforcement at the maximum load level as is necessary to establish the bond provision for plain bars in terms of lap splice and

development length. The investigation described herein therefore extends the previous studies conducted at the University of Saskatchewan to ultimately propose equations for inclusion in a future edition of the ACI 562 code. Current code provisions for the development and lap splice length of deformed bars were established using a statistical analysis of data obtained from test results of splice and beam-end specimens by Orangun et al. (1977). A similar approach is being used for the plain bar in the current experimental program.

It is important to address the post-yield behaviour of specimens reinforced with plain bars before a code equation is proposed as the degree of ductility results in significant differences in structural behaviour. Bischoff and Johnson (2008) tested four specimens to compare the bond behaviour of plain and deformed bars. They reported that specimens with deformed bars showed a large yield plateau before failure while specimens with plain bars failed without any significant yield plateau once the proportional limit of the reinforcing steel was exceeded. However, proposed code equations for plain bars can only be developed in a similar manner, with a similar level of safety as those developed for deformed bars, if a ductile failure is observed. Two specimens with lap splice lengths longer than that predicted to allow for yielding of the reinforcement were therefore included in this investigation.

This paper presents the results of the extended experimental program and outlines the analysis required to determine the tensile resistance of the spliced longitudinal reinforcement at the maximum attained load level as a basis for establishing development length criteria for plain bars.

2 Experimental Program

The description of the specimens and test setups are similar to those reported by Hassan and Feldman (2012) and Sekulovic Maclean and Feldman (2014). Figure 1 shows the cross-section, elevation, and plan view for the 35 specimens included in this study. All of these specimens have identical cross-section and span length. Table 1 shows that 12 of the specimens were originally reported by Hassan and Feldman (2012) and 15 of the specimens were originally reported by Sekulovic MacLean and Feldman (2014).

The splice specimens were constructed with either the round or square spliced longitudinal bars cast in bottom (Figure 1(a)) or top position (Figure 1(b)), respectively. The 50 mm clear concrete cover all around was held constant for all of the specimens. The effective depth of the reinforcement, *d,* was 350, 347 and 344 mm for specimens reinforced with 19, 25 and 32 mm bars, respectively. Specimens that were cast with the spliced reinforcing bars in the top position were inverted before testing.

Figure 1(c) shows the elevation of all specimens at testing, and Figure 1(d) shows the plan view of the specimens with the arrangement of the spliced reinforcement. The shear span to depth ratio, *a/d*, for all specimens is around 3.94. All specimens were designed to fail in bond with the exception of specimens reinforced with 19 mm round bars and lap splice lengths, L_s, of 1010 mm and 1210 mm. These specimens were intentionally designed to fail in flexure. With these two exceptions, lap splice lengths, L_s, varied from 12.8 to 19.1 times the bar size. A vertical load, *P,* was applied via a single actuator at a rate of 0.0015 mm/s to failure. A spreader beam with a self-weight of 1.77 kN was used to distribute this load to two points located 915 mm on either side of the specimen centreline to establish the four-point loading arrangement (Figure 1(c)).

2.1 Concrete

The target concrete compressive strength was 20MPa. General purpose (Type GU) Portland cement was used without admixtures. Two mix designs were used as indicated in Table 1 due to a change in material supplier partway through this multi-year investigation. Mix design #1 (per m^3 of concrete) consisted of: 250 g cement, 110 kg crushed limestone and granite coarse aggregate blend, 1100 kg silica sand fine aggregate and 140 L water. Mix design #2 consisted of a carbonate gneiss and granite coarse aggregate blend, and a washed silica sand fine aggregate. The mix design per m^3 of concrete consisted of: 270 kg cement, 993 kg sand, 1039 kg crushed coarse aggregate, and 145 L water. The maximum aggregate size for both mixes was 20 mm and all aggregates conformed to CAN/CSA A23.1-09 (2009).

Table 1: Results of Lap Splice Specimens

Specimen Identification[a]	Splice Length as a Function of Bar Size (L_s/d_b)	Concrete Compressive Strength f'_c (MPa)	Maximum Normalized Load, $P_{max}/\sqrt{f'_c}$ kN/√MPa	Predicted Normalized Maximum Load $P_{max}/\sqrt{f'_c}$ kN/√MPa	Tension in the Reinforcement at the Maximum Load (kN)
19●-305↓[b]	16.1	17.4[d]	8.50	18.0	105
19●-410↓[b]	21.6	17.4[d]	9.14	18.0	110
19●-510↓[b]	26.8	18.7[d]	9.58	17.5	117
19●-610↓[b]	32.1	21.0[d]	17.8	16.7	n/a
19●-1010↓	53.2	23.8[e]	23.6	15.3	n/a
19●-1210↓	63.7	20.3[e]	22.0	16.4	n/a
25●-410↓[b]	16.4	23.7[d]	16.2	28.1	204
25●-510↓[b]	20.4	24.0[d]	18.4	27.7	230
25●-610↓[b]	24.4	22.8[d]	20.6	28.5	249
25●-810↓[b]	32.4	19.2[d]	29.7	30.3	325
25●-410↑[c]	16.4	27.1[e]	6.55	28.1	105
25●-510↑[c]	20.4	28.0[e]	4.69	27.7	84.5
25●-610↑[c]	24.4	35.8[e]	7.07	25.1	122
32●-410↓[b]	12.8	19.8[d]	15.6	44.5	191
32●-610↓[b]	19.1	19.8[d]	25.1	44.3	291
32●-810↓[b]	25.3	15.8[d]	31.8	46.9	330
32●-910↓[b]	28.4	19.7[d]	34.5	45.8	n/a
19■-410↓	21.6	24.7[e]	15.8	19.8	197
19■-510↓	26.8	22.8[e]	23.1	20.5	n/a
19■-610↓	32.1	22.7[e]	24.2	20.6	n/a
19■-410↑	21.6	22.9[e]	9.74	20.5	128
19■-510↑	26.8	23.0[e]	9.36	20.4	124
19■-610↑	32.1	24.6[e]	14.3	20.6	180
25■-410↓[c]	16.4	25.5[e]	16.1	38.3	212
25■-510↓[c]	20.4	25.0[e]	20.0	38.3	255
25■-610↓[c]	24.4	28.1[e]	26.8	36.6	349
25■-410↑[c]	16.4	33.0[e]	8.97	31.3	142
25■-510↑[c]	20.4	33.5[e]	11.2	31.1	174
25■-610↑[c]	24.4	33.0[e]	12.2	31.3	186
32■-410↓[c]	12.8	25.5[e]	17.4	50.6	235
32■-610↓[c]	19.1	25.5[e]	20.1	50.8	268
32■-810↓[c]	25.3	26.9[e]	28.3	49.5	373
32■-410↑[c]	12.8	27.5[e]	12.6	49.4	183
32■-610↑[c]	19.1	26.2[e]	14.3	50.4	201
32■-810↑[c]	25.3	26.2[e]	16.2	50.4	224

[a]Specimen designations consist of two numbers and associated symbols separated by a hyphen. The first number represents the nominal diameter for round bars or side face dimension for square bars in millimeters; a solid circle (●) or solid square (■) represents the shape of reinforcement; the number following the hyphen represents lap splice length in millimeters, with an arrow sign representing the position of reinforcing bar during casting in which a downward arrow (↓) represents the bottom position and an upward arrow (↑) represents the top position.
[b]Originally reported by Hassan and Feldman (2012)
[c]Originally reported by Sekulovic MacLean and Feldman (2014)
[d]Specimens cast with Concrete Mix Design 1
[e]Specimens cast with Concrete Mix Design 2.

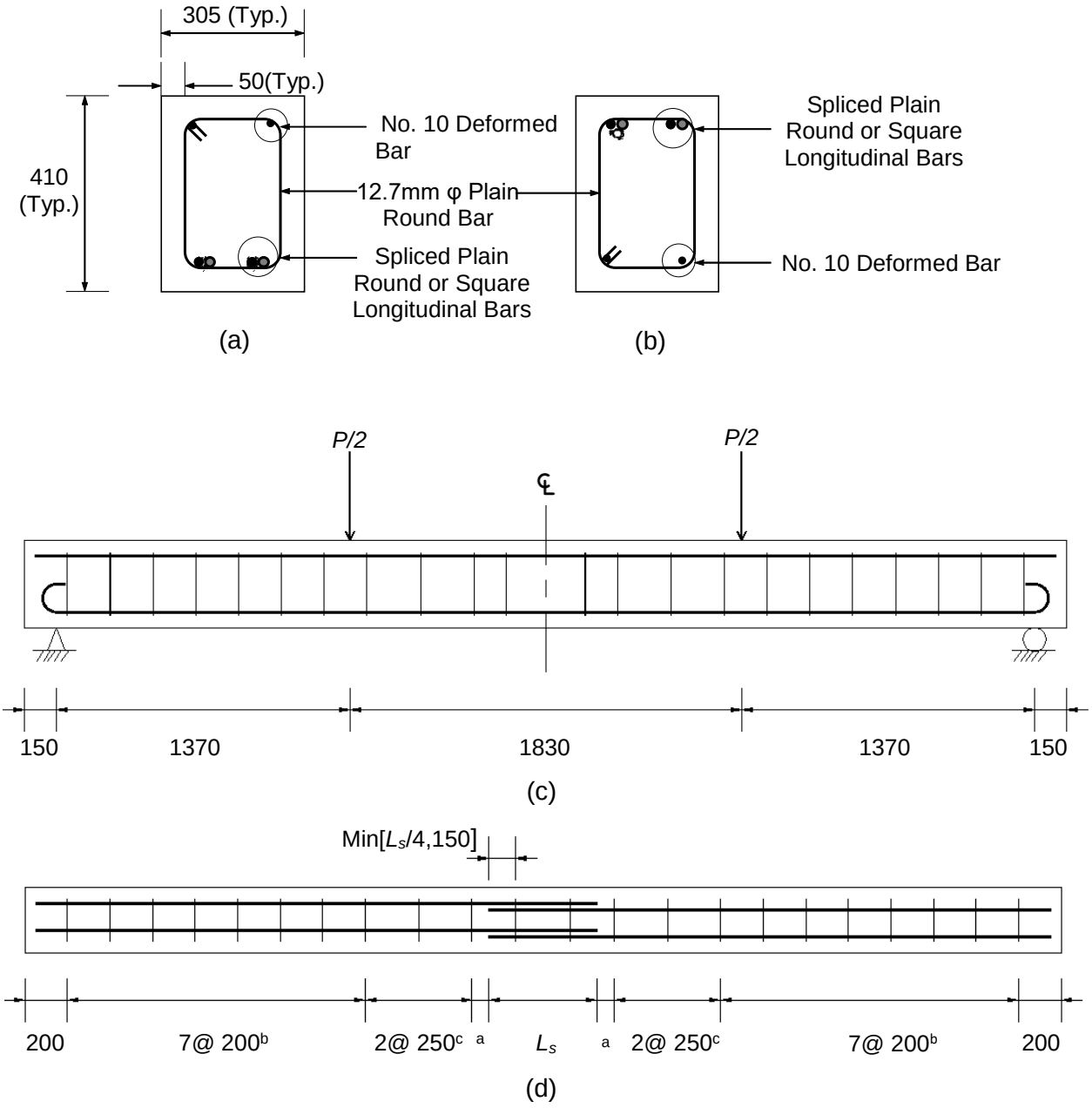

Notes:
[a]Varies with splice length
[b]7@ 200 for L_s < 1210 mm;8@ 200 for L_s 1210 mm
[c] 2 Spaces for L_s < 810 mm; 1 space for L_s 810 mm and 1010 mm; n/a for L_s 1210 mm

Figure 1: Splice Specimen Geometry: (a) Cross-Section for Specimens with Bottom-Cast Spliced Longitudinal Reinforcement, (b) Cross-Section for Specimens with Top-Cast Spliced Longitudinal Reinforcement, (c) Elevation, and (d) Plan View.

The concrete compressive strength of the specimens at the time of testing was established from companion tests conducted on the same day as the corresponding lap splice specimen and are reported in Table 1. These companion concrete cylinders were 100 mm in diameter and 200 mm long and were stored under the same conditions as the corresponding splice specimen. Specimens were moist cured using wet burlap and plastic sheets for 7 days following casting, and were then stored in the laboratory until testing.

2.2 Reinforcement

All principal longitudinal reinforcement was hot-rolled CSA G40.21 300W steel. One hundred and eighty-degree hooks were provided at the ends adjacent to each beam support to ensure that failure occurred within the lap splice length. The material properties of the longitudinal reinforcement were evaluated using companion tensile strength tests of excess bar lengths. Table 2 shows the static yield strength, f_{ys}, calculated in accordance with Rao et al. (1966); the dynamic yield strength, f_{yd}; the ultimate strength, f_u; and the modulus of elasticity, E_s; for all of the spliced longitudinal bars.

The surface roughness of the lap spliced plain bars was increased by sandblasting techniques to make them more representative of historical bars (Feldman and Bartlett, 2005). This was done by using 220-grit aluminium oxide, a nozzle distance of 125 mm and a blast pressure of 698 kPa. A total of around 30 to 40 roughness measurements were made on each bar using a surface roughness tester and a single 0.25 mm stroke. The distance between the highest peak and deepest indention on the surface, R_y, within the stroke length characterized the surface roughness of each bar (Mitutoyo, 2006). The average combined R_y value for all longitudinal bars was 9.26 µm.

The shear reinforcement was 12.7 mm diameter hot-rolled CSA G40.21 300W plain steel bars. Figure 1(d) shows that these bars were spaced at 200 mm on center in the shear spans and typically at 250 mm on center within the constant moment region, where applicable, as shown in Figure 1(d). In order to prevent prying action of the longitudinal reinforcement, two additional stirrups were provided in the splice region which were placed at minimum of one-quarter of the splice length or 150mm from each end of the splice. More shear reinforcement than necessary was provided to ensure that a shear failure did not govern. Grade 400 deformed reinforcing bars were used to facilitate the assembly of the reinforcement cage.

Table 2: Mechanical Properties of the Spliced Longitudinal Reinforcement

Bar Identification	Static Yield Strength f_{ys}, *MPa*	Dynamic Steel Strength f_{yd}, *MPa*	Ultimate Strength f_{ud}, *MPa*	Modulus of Elasticity E_s, *GPa*
19●↓[a]	326	355	520	203
19●↓[b]	315	336	520	196
25●↓[c]	322	346	534	196
25●↓[d]	316	346	504	206
25●↑	334	364	522	243
32●↓	318	348	504	204
19■↓ and 19■↑	320	350	522	162
25■↓	349	381	544	192
25■↑	316	349	542	207
32■↓ and 32■↑	312	343	527	196

[a] Specimens with lap splice lengths equal to 305, 410, 510 and 610 mm
[b] Specimens with lap splice lengths equal to 1010 and 1210 mm
[c] Specimens with lap splice lengths equal to 410, 510 and 610 mm
[d] Specimens with lap splice lengths equal to 810 mm

3 Test Results and Analysis

Table 1 shows the maximum recorded loads attained by the specimens and those predicted assuming yielding of the reinforcement without strain hardening. The weight of the spreader beam (1.77 kN) and self-weight of the specimen (2.94 kN/m) were subtracted when calculating predicted maximum load. All reported loads have been normalized by the square root of the concrete compressive strength, as was shown to reasonably represent the concrete contribution to bond strength by Orangun et al. (1977) for values of f'_c less than 55 MPa, to allow for a direct comparison between the specimens.

Two specimens (19●-1010↓ and 19●-1210↓) were intentionally cast with lap splice lengths longer than that which would cause yielding of the reinforcement. Table 1 shows that these specimens failed at loads above the yield loads predicted using the flexural resistance procedures provided in CSA A23.3 (2014) with resistance factors set equal to unity. Figure 2 shows that the load versus deflection behaviour of these specimens includes a long yield plateau and hence suggests that proposed code equations for the development of plain bars can be developed in a similar manner with a similar level of safety as those developed for deformed bars. In contrast with Bischoff and Johnson's (2008) findings, the load deflection behaviour observed in this experimental program therefore suggests that failure was ductile in nature.

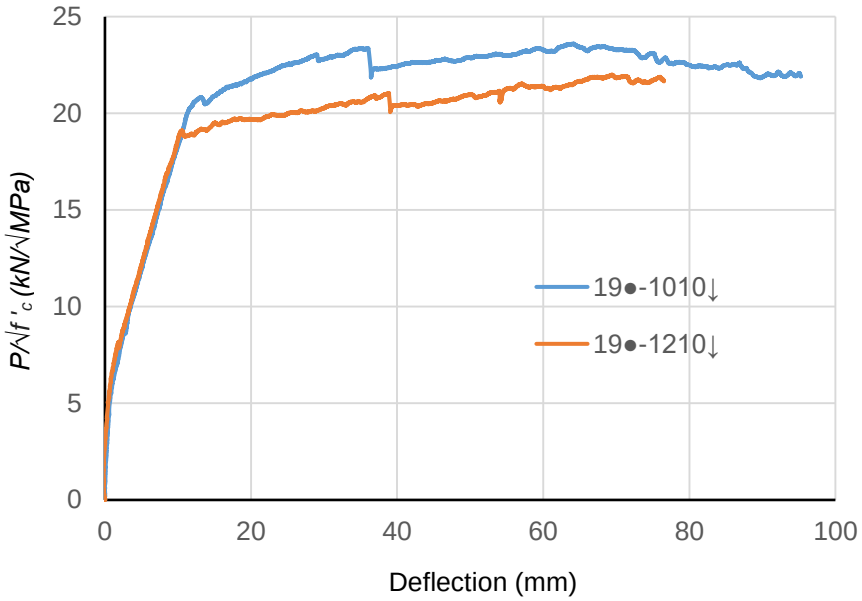

Figure 2: Normalized applied load versus midspan deflection for specimens with lap splice lengths greater than that anticipated to cause yielding of the reinforcement

Table 1 shows that Specimens 19●-610↓, 19■-510↓ and 19■-610↓ failed at loads greater than that predicted to cause yielding of the reinforcement. Based upon a review of the measured load deflection behaviour, it would appear that Specimens 19●-610↓and 19■-510↓ failed in bond as a yield plateau was not evident upon review of the load versus deflection data for these specimens, whereas Specimen 19■-610↓ appeared to fail in flexure as a yield plateau was evident for this specimen. Specimen 32●-910↓ was identified as a physical outlier due to the technical errors encountered during testing. This specimen required unloading and loading twice prior to failure resulting in large plastic deformations between the load cycles. All of these specimens (19●-610↓, 19■-510↓,19■-610↓ and 32●-910↓) will be excluded from the subsequent analysis and test database used to establish proposed code provisions for lap splice and development length.

3.1 Moment Curvature Analysis

A moment curvature analysis was performed to calculate the tensile resistance of the reinforcement at the maximum load level. A direct measurement of the tension in the reinforcement is not possible without compromising the bond between the spliced longitudinal reinforcing bars and surrounding concrete. In the analysis, the moment versus curvature response is calculated and plotted from the initial condition (i.e. prior to loading being applied) to the maximum specimen capacity.

The stress-strain relationship for the concrete was modelled using a Hognestad equation (Hognestad, 1951):

[1] $\frac{f_c}{f'_c} = \left[2\left(\frac{\varepsilon_c}{\varepsilon_o}\right) - \left(\frac{\varepsilon_c}{\varepsilon_o}\right)^2 \right]$ for $\varepsilon_c < \varepsilon_o$

[2] $\frac{f_c}{f'_c} = \left[1 - \frac{0.15(\varepsilon_c - \varepsilon_o)}{0.0038 - \varepsilon_o} \right]$ for $\varepsilon_c > \varepsilon_o$

where f_c is the compressive stress in the concrete at any given location along the height of the cross-section, ε_c is the concrete stain corresponding to f_c, and ε_o is the strain corresponding to the maximum compressive stress of concrete and is defined as:

[3] $\varepsilon_o = \frac{2f'_c}{E_c}$

where E_c is the modulus of elasticity of the concrete.

The stress versus strain relationship for the reinforcement was modelled using a three-phased approach: (1) a linear segment to represent the elastic region, (2) a horizontal line to represent the yield plateau, and (3) a best fit cubic equation to represent the strain hardening region of the stress versus strain response of the reinforcement. As-measured tensile properties of the reinforcement as shown in Table 2 were used to establish the theoretical stress-strain curve.

The moment versus curvature of the uncracked section was established by using simple flexural formula in which the resisting moment was set equal to the product of curvature and flexural rigidity, *EI*, of the gross section. For the cracked section, an iterative procedure was applied in which the compressive stress block was divided into 100 segments of equal depth, with the magnitude of the stress in each segment assumed equal to that at the midheight of the segment. Figure 3 shows the procedure used for the sectional analysis of the specimens used to establish moment curvature relationship for the cracked section. A linear strain profile as shown in Figure 3(a) was assumed and similar triangles were used to calculate the strain in the reinforcing steel, ε_s, at the centre of each of the 100 compression segments, ε_i. The compressive force in each of the 100 segments, C_i, was obtained by first determining the compressive stress, $f_c(\varepsilon_i)$, corresponding to the strain ε_i in the given segment as shown in Figures 3(a) and (b). The compressive stress was then multiplied by the cross-sectional area of the segment which is equal to the product of the width of specimen, *b*, and the thickness of each segment. The thickness of each segment was set equal to *c*/100. The total compressive force in the cross-section, *C*, was then calculated by summing the compressive force in all of the segments as shown in Figure 3(c). The tensile force in the cross section, *T*, was obtained by first determining the tensile stress of reinforcement, corresponding to the calculated strain ε_s, at the centroid of the lapped longitudinal bars as shown in Figures 3(a) and (b). The total tensile force in the cross section, *T*, was then calculated by multiplying cross-sectional area of the reinforcement by the tensile stress. The neutral axis depth, *c*, for the cross-section was then established at a given curvature based on horizontal equilibrium such that the compressive force, *C*, of the concrete was equal to the tensile force, *T*, in the longitudinal reinforcement within a 0.5% tolerance level. Finally, the resisting moment was calculated as the product of the tensile force in the lapped bars and the lever arm (i.e. distance between centroid of compressive and tensile force).

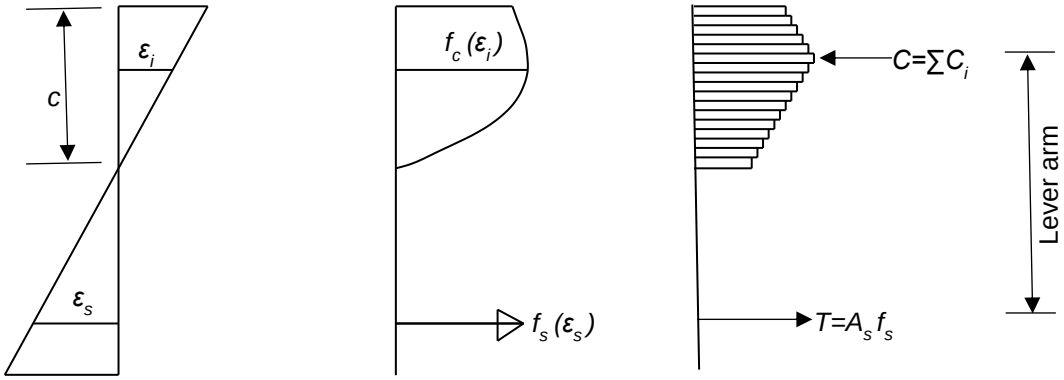

Figure 3: Graphical description of the moment curvature analysis (a) strain distribution (b) stress distribution and (c) force distribution acting on the cross-section of the specimen

Figure 4 shows the moment versus curvature diagram for Specimen 19●-305↓. The moment at the maximum load was calculated using statics. The curvature corresponding to the maximum moment was then determined graphically from the moment curvature diagram. The tensile resistance of the reinforcement at the maximum load was calculated from the curvature as described in the previous paragraph.

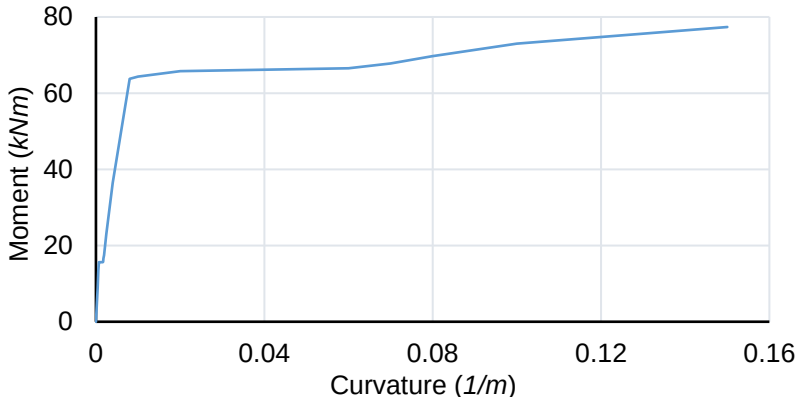

Figure 4: Moment curvature diagram for Specimen 19●-305↓

Table 1 shows the tensile resistance of the reinforcement at the maximum load for each specimen as calculated from the moment curvature analysis. It is to be noted that the tensile resistance of reinforcement is reported for the total of the two lap spliced bars in each specimen. Lap splice and development length provisions for plain bars can be established by performing a regression analysis of the tensile resistance of the reinforcement at the maximum load level as a function of bar size, lap splice length, and casting position using a similar procedure as that reported by Orangun et al. (1977) for deformed bars.

The error in the calculated moments corresponding to a given curvature based on the selection of 100 segments was evaluated. Figure 5 shows the moment corresponding to a fixed curvature of 0.0035/m for Specimen 19●-305↓ as calculated for 2, 5, 10, 20, 50, 100, 200, 300, 400 and 500 segments. The curvature value of 0.0035/m was selected arbitrarily such that it was located in the linear segment of the moment-curvature diagram prior to yielding of the reinforcement. When the number of segments considered in the analysis was greater than or equal to 300, the moment closely approached the constant value of 32.0133 kNm. Hence the asymptote was reported as that value as shown in Figure 5. The error associated with the selection of 100 segments was therefore negligible.

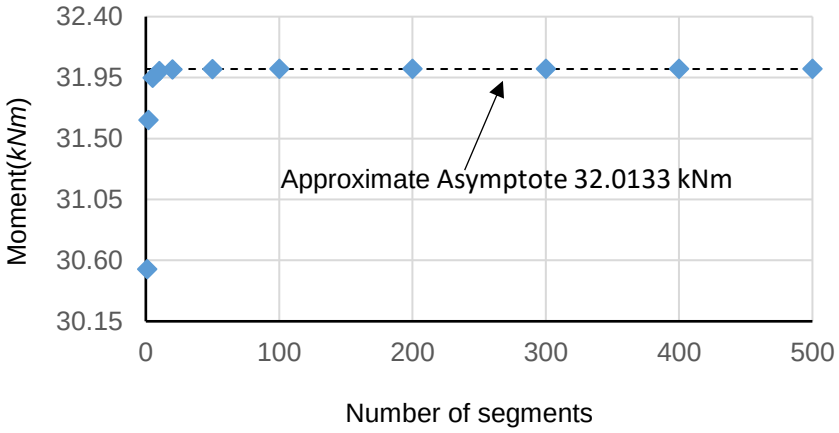

Figure 5: Moment corresponding to a curvature of 0.0035/m as a function of the number of segments incorporated in the analysis of Specimen 19●-305↓

Figure 6 shows a comparison of the tensile resistance of the reinforcement at the maximum load level as calculated from two different methods. In Method A, the tensile resistance was calculated from the resisting moment as a product of the tensile force in the spliced longitudinal reinforcement and the lever arm (i.e. distance between the centroid of tension force and the centroid of compression force in the concrete above the neutral axis); whereas in Method B, the tensile resistance was calculated from the resisting moment as a product of compressive force in the concrete above the neutral axis location and the same lever arm. The mean and standard deviation of the ratio of the tensile resistance as calculated from Methods A and B are 0.98 and 0.003, respectively. Method B generally gave slightly greater values for the tensile resistance than Method A because the neutral axis depth was calculated iteratively from a higher to a lower value until the difference between the compressive force in the concrete and the tensile force in the reinforcement was within 0.5%. Method A was therefore chosen as it generally yielded slightly lower values for the tensile resistance in the lap spliced longitudinal bars which would translate to longer lap splice lengths.

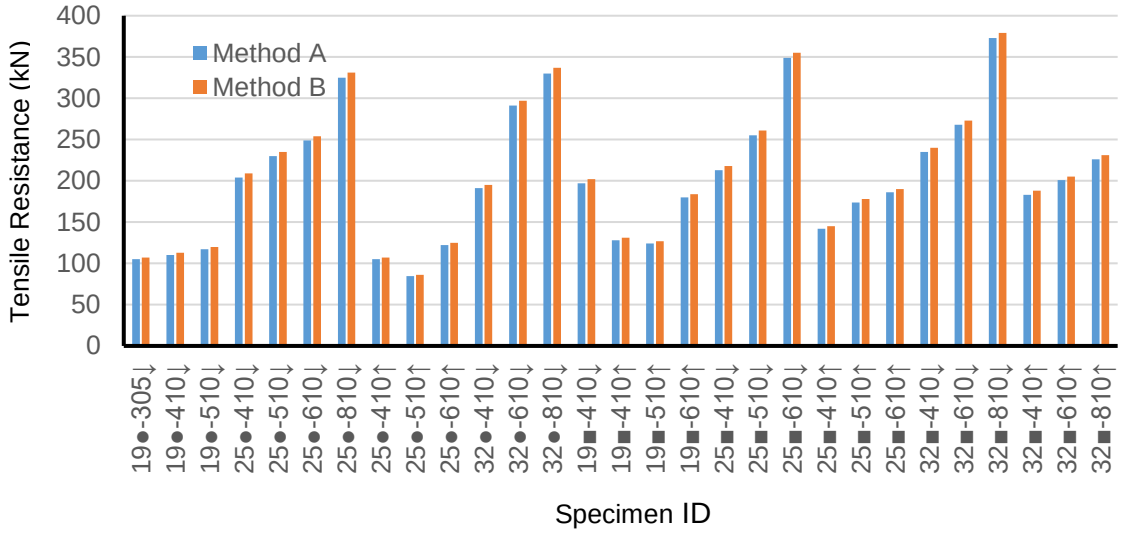

Note: Specimens that are designed to fail in flexure (i.e. 19●-1010↓ and 19●-1210↓), specimens that failed at load above the maximum predicted load (19●-610↓, 19■-510↓ and 19■-610↓) and physical outlier (32●-910↓) are not shown

Figure 6: Comparison of two different methods for calculating the tensile resistance of the spliced reinforcement at the maximum load

4 Summary and Conclusions

This paper presents the results of an experimental investigation consisting of 35 splice specimens reinforced with plain bars that were subjected to four-point loading. Specimens were cast with either plain round or square bars cast either in the bottom or top position. All specimens had similar geometry with a span length of 4870mm, a width of 305mm, and a height of 410mm. Lap splice lengths varied from 12.8 to 32.1 times the bar size for the specimens that were designed to fail in bond. Two specimens with lap splice lengths long enough to produce yielding of the reinforcement were also cast to confirm the nature of the resulting failure. The following significant conclusions are noted:

1. The nature of failure of specimens with long splice lengths is ductile with a long yield plateau.
2. The tensile resistance of the longitudinal reinforcement at the maximum load was determined from a moment curvature analysis. The error associated with the selection of 100 segments within the compression zone is close to zero percent.
3. Lap splice and development length provisions for plain bars can be established by performing a regression analysis of the tensile resistance of the reinforcement at the maximum load as a function of lap splice length, bar diameter, and casting position.

Acknowledgements

The authors would like to gratefully acknowledge the assistance of Brennan Pokoyoway and Dale Pavier, structures laboratory technicians, for preparation and testing of the specimens. The authors would also like to thank Lafarge Canada Inc. for supplying ready mix concrete in-kind. Financial support was provided by the Natural Science and Engineering Research Council of Canada, and the Saskatchewan Centre of Excellence for Transportation and Infrastructure. Scholarship support for the first author was also provided by the University of Saskatchewan.

References

Baldwin, M.I. and Clark, L.A. 1995. The Assessment of Reinforcing Bars with Inadequate Anchorage. *Magazine of Concrete Research,* **47**(171):95-102.

Bischoff, P.H. and Johnson, R.D. 2008. Effect of Bond and Cracking on Serviceability Related Behaviour of Concrete Beams Reinforced with Plain (Undeformed) Reinforcing Bars. *Canadian Society of Civil Engineering, 37th Annual Conference*, Quebec, QC, Canada

CSA. 2009. CAN/CSA A23.1/A23.2-09 *Concrete Materials and Concrete Construction/Test Methods and Standard Practises for Concrete*, Canadian Standards Association, Mississauga, ON, Canada.

CSA. 2014. *CAN/CSA A23.3-14 Design of Concrete Structures*, Canadian Standards Association, Mississauga, ON.

Edwards A. D. and Yannopoulos P. J. 1979. Local Bond-Stress to Slip Relationships for Hot Rolled Deformed Bars and Mild Steel Plain Bars. *ACI Structural Journal*, **76**(3):405-420.

Feldman, L.R. and Bartlett, F.M. 2005. Bond Strength Variability in Pullout Specimens with Plain Reinforcement. *ACI Structural Journal*, **102**(6):860-867.

Hassan, M.N. and Feldman, L.R. 2012. Behaviour of Lap Spliced Plain Steel Bars. *ACI Structural Journal*, **109**(2):235-243.

Hognestad, E. 1951. A Study of Combined Bending and Axial Load in Reinforced Concrete Members. *University of Illinois Engineering Experimental Station, Bulletin Series No. 399.*

Idun, E.K., and Darwin, D. 1995. *Improving the Development Characteristics of Steel Reinforcing Bars*. SM Report No. 41, University of Kansas Centre for Research, Lawrence, Kansas, U.S.A.

Mitutoyo, 2006. *SJ-201 Surface Roughness Tester User's Manual No.99MBB0796A*. Mitutoyo Corporation, Kanagawa, Japan.

Orangun, C.O., Jirsa, J.O., and Breen, J.E. 1977. Re-Evaluation of Test Data on Development Length and Splices. *ACI Journal*, **74**(3):114-122.

Rao, N. R.M, Lohrmann, M. and Tall, L. 1966. Effects of Strain Rate on the Yield Stress of Structural Steels. *ASTM Journal of Materials*, **1** (1): 241-262.

Sekulovic MacLean, M. and Feldman, L.R. 2014. Effects of Casting Position and Bar Shape on Bond of Plain Bars. *ACI Structural Journal*, **111**(2):323-330.